Fermilab FERMILAB-Pub-01/290-E D0 Oct. 2001

The Inclusive Jet Cross Section in $p\overline{p}$ Collisions at $\sqrt{s} = 1.8$ TeV using the $k_\perp$ Algorithm

V.M. Abazov,[23] B. Abbott,[57] A. Abdesselam,[11] M. Abolins,[50] V. Abramov,[26] B.S. Acharya,[17] D.L. Adams,[59] M. Adams,[37] S.N. Ahmed,[21] G.D. Alexeev,[23] A. Alton,[49] G.A. Alves,[2] N. Amos,[49] E.W. Anderson,[42] Y. Arnoud,[9] C. Avila,[5] M.M. Baarmand,[54] V.V. Babintsev,[26] L. Babukhadia,[54] T.C. Bacon,[28] A. Baden,[46] B. Baldin,[36] P.W. Balm,[20] S. Banerjee,[17] E. Barberis,[30] P. Baringer,[43] J. Barreto,[2] J.F. Bartlett,[36] U. Bassler,[12] D. Bauer,[28] A. Bean,[43] F. Beaudette,[11] M. Begel,[53] A. Belyaev,[35] S.B. Beri,[15] G. Bernardi,[12] I. Bertram,[27] A. Besson,[9] R. Beuselinck,[28] V.A. Bezzubov,[26] P.C. Bhat,[36] V. Bhatnagar,[15] M. Bhattacharjee,[54] G. Blazey,[38] F. Blekman,[20] S. Blessing,[35] A. Boehnlein,[36] N.I. Bojko,[26] F. Borcherding,[36] K. Bos,[20] T. Bose,[52] A. Brandt,[59] R. Breedon,[31] G. Briskin,[58] R. Brock,[50] G. Brooijmans,[36] A. Bross,[36] D. Buchholz,[39] M. Buehler,[37] V. Buescher,[14] V.S. Burtovoi,[26] J.M. Butler,[47] F. Canelli,[53] W. Carvalho,[3] D. Casey,[50] Z. Casilum,[54] H. Castilla-Valdez,[19] D. Chakraborty,[38] K.M. Chan,[53] S.V. Chekulaev,[26] D.K. Cho,[53] S. Choi,[34] S. Chopra,[55] J.H. Christenson,[36] M. Chung,[37] D. Claes,[51] A.R. Clark,[30] L. Coney,[41] B. Connolly,[35] W.E. Cooper,[36] D. Coppage,[43] S. Crépé-Renaudin,[9] M.A.C. Cummings,[38] D. Cutts,[58] G.A. Davis,[53] K. Davis,[29] K. De,[59] S.J. de Jong,[21] K. Del Signore,[49] M. Demarteau,[36] R. Demina,[44] P. Demine,[9] D. Denisov,[36] S.P. Denisov,[26] S. Desai,[54] H.T. Diehl,[36] M. Diesburg,[36] S. Doulas,[48] Y. Ducros,[13] L.V. Dudko,[25] S. Duensing,[21] L. Duflot,[11] S.R. Dugad,[17] A. Duperrin,[10] A. Dyshkant,[38] D. Edmunds,[50] J. Ellison,[34] J.T. Eltzroth,[59] V.D. Elvira,[36] R. Engelmann,[54] S. Eno,[46] G. Eppley,[61] P. Ermolov,[25] O.V. Eroshin,[26] J. Estrada,[53] H. Evans,[52] V.N. Evdokimov,[26] T. Fahland,[33] S. Feher,[36] D. Fein,[29] T. Ferbel,[53] F. Filthaut,[21] H.E. Fisk,[36] Y. Fisyak,[55] E. Flattum,[36] F. Fleuret,[12] M. Fortner,[38] H. Fox,[39] K.C. Frame,[50] S. Fu,[52] S. Fuess,[36] E. Gallas,[36] A.N. Galyaev,[26] M. Gao,[52] V. Gavrilov,[24] R.J. Genik II,[27] K. Genser,[36] C.E. Gerber,[37] Y. Gershtein,[58] R. Gilmartin,[35] G. Ginther,[53] B. Gómez,[5] G. Gómez,[46] P.I. Goncharov,[26] J.L. González Solís,[19] H. Gordon,[55] L.T. Goss,[60] K. Gounder,[36] A. Goussiou,[28] N. Graf,[55] G. Graham,[46] P.D. Grannis,[54] J.A. Green,[42] H. Greenlee,[36] Z.D. Greenwood,[45] S. Grinstein,[1] L. Groer,[52] S. Grünendahl,[36] A. Gupta,[17] S.N. Gurzhiev,[26] G. Gutierrez,[36] P. Gutierrez,[57] N.J. Hadley,[46] H. Haggerty,[36] S. Hagopian,[35] V. Hagopian,[35] R.E. Hall,[32] P. Hanlet,[48] S. Hansen,[36] J.M. Hauptman,[42] C. Hays,[52] C. Hebert,[43] D. Hedin,[38] J.M. Heinmiller,[37] A.P. Heinson,[34] U. Heintz,[47] M.D. Hildreth,[41] R. Hirosky,[62] J.D. Hobbs,[54] B. Hoeneisen,[8] Y. Huang,[49] I. Iashvili,[34] R. Illingworth,[28] A.S. Ito,[36] M. Jaffré,[11] S. Jain,[17] R. Jesik,[28] K. Johns,[29] M. Johnson,[36] A. Jonckheere,[36] H. Jöstlein,[36] A. Juste,[36] W. Kahl,[44] S. Kahn,[55] E. Kajfasz,[10] A.M. Kalinin,[23] D. Karmanov,[25] D. Karmgard,[41] R. Kehoe,[50] A. Khanov,[44] A. Kharchilava,[41] S.K. Kim,[18] B. Klima,[36] B. Knuteson,[30] W. Ko,[31] J.M. Kohli,[15] A.V. Kostritskiy,[26] J. Kotcher,[55] B. Kothari,[52] A.V. Kotwal,[52] A.V. Kozelov,[26] E.A. Kozlovsky,[26] J. Krane,[42] M.R. Krishnaswamy,[17] P. Krivkova,[6] S. Krzywdzinski,[36] M. Kubantsev,[44] S. Kuleshov,[24] Y. Kulik,[54] S. Kunori,[46] A. Kupco,[7] V.E. Kuznetsov,[34] G. Landsberg,[58] W.M. Lee,[35] A. Leflat,[25] C. Leggett,[30] F. Lehner,[36,*] C. Leonidopoulos,[52] J. Li,[59] Q.Z. Li,[36] X. Li,[4] J.G.R. Lima,[3] D. Lincoln,[36] S.L. Linn,[35] J. Linnemann,[50]

R. Lipton,[36] A. Lucotte,[9] L. Lueking,[36] C. Lundstedt,[51] C. Luo,[40] A.K.A. Maciel,[38] R.J. Madaras,[30] V.L. Malyshev,[23] V. Manankov,[25] H.S. Mao,[4] T. Marshall,[40] M.I. Martin,[38] K.M. Mauritz,[42] A.A. Mayorov,[40] R. McCarthy,[54] T. McMahon,[56] H.L. Melanson,[36] M. Merkin,[25] K.W. Merritt,[36] C. Miao,[58] H. Miettinen,[61] D. Mihalcea,[38] C.S. Mishra,[36] N. Mokhov,[36] N.K. Mondal,[17] H.E. Montgomery,[36] R.W. Moore,[50] M. Mostafa,[1] H. da Motta,[2] E. Nagy,[10] F. Nang,[29] M. Narain,[47] V.S. Narasimham,[17] N.A. Naumann,[21] H.A. Neal,[49] J.P. Negret,[5] S. Negroni,[10] T. Nunnemann,[36] D. O'Neil,[50] V. Oguri,[3] B. Olivier,[12] N. Oshima,[36] P. Padley,[61] L.J. Pan,[39] K. Papageorgiou,[37] A. Para,[36] N. Parashar,[48] R. Partridge,[58] N. Parua,[54] M. Paterno,[53] A. Patwa,[54] B. Pawlik,[22] J. Perkins,[59] O. Peters,[20] P. Pétroff,[11] R. Piegaia,[1] B.G. Pope,[50] E. Popkov,[47] H.B. Prosper,[35] S. Protopopescu,[55] M.B. Przybycien,[39,†] J. Qian,[49] R. Raja,[36] S. Rajagopalan,[55] E. Ramberg,[36] P.A. Rapidis,[36] N.W. Reay,[44] S. Reucroft,[48] M. Ridel,[11] M. Rijssenbeek,[54] F. Rizatdinova,[44] T. Rockwell,[50] M. Roco,[36] C. Royon,[13] P. Rubinov,[36] R. Ruchti,[41] J. Rutherfoord,[29] B.M. Sabirov,[23] G. Sajot,[9] A. Santoro,[2] L. Sawyer,[45] R.D. Schamberger,[54] H. Schellman,[39] A. Schwartzman,[1] N. Sen,[61] E. Shabalina,[37] R.K. Shivpuri,[16] D. Shpakov,[48] M. Shupe,[29] R.A. Sidwell,[44] V. Simak,[7] H. Singh,[34] J.B. Singh,[15] V. Sirotenko,[36] P. Slattery,[53] E. Smith,[57] R.P. Smith,[36] R. Snihur,[39] G.R. Snow,[51] J. Snow,[56] S. Snyder,[55] J. Solomon,[37] Y. Song,[59] V. Sorín,[1] M. Sosebee,[59] N. Sotnikova,[25] K. Soustruznik,[6] M. Souza,[2] N.R. Stanton,[44] G. Steinbrück,[52] R.W. Stephens,[59] F. Stichelbaut,[55] D. Stoker,[33] V. Stolin,[24] A. Stone,[45] D.A. Stoyanova,[26] M.A. Strang,[59] M. Strauss,[57] M. Strovink,[30] L. Stutte,[36] A. Sznajder,[3] M. Talby,[10] W. Taylor,[54] S. Tentindo-Repond,[35] S.M. Tripathi,[31] T.G. Trippe,[30] A.S. Turcot,[55] P.M. Tuts,[52] V. Vaniev,[26] R. Van Kooten,[40] N. Varelas,[37] L.S. Vertogradov,[23] F. Villeneuve-Seguier,[10] A.A. Volkov,[26] A.P. Vorobiev,[26] H.D. Wahl,[35] H. Wang,[39] Z.-M. Wang,[54] J. Warchol,[41] G. Watts,[63] M. Wayne,[41] H. Weerts,[50] A. White,[59] J.T. White,[60] D. Whiteson,[30] D.A. Wijngaarden,[21] S. Willis,[38] S.J. Wimpenny,[34] J. Womersley,[36] D.R. Wood,[48] Q. Xu,[49] R. Yamada,[36] P. Yamin,[55] T. Yasuda,[36] Y.A. Yatsunenko,[23] K. Yip,[55] S. Youssef,[35] J. Yu,[36] Z. Yu,[39] M. Zanabria,[5] X. Zhang,[57] H. Zheng,[41] B. Zhou,[49] Z. Zhou,[42] M. Zielinski,[53] D. Zieminska,[40] A. Zieminski,[40] V. Zutshi,[55] E.G. Zverev,[25] and A. Zylberstejn[13]

(DØ Collaboration)

[1] *Universidad de Buenos Aires, Buenos Aires, Argentina*
[2] *LAFEX, Centro Brasileiro de Pesquisas Físicas, Rio de Janeiro, Brazil*
[3] *Universidade do Estado do Rio de Janeiro, Rio de Janeiro, Brazil*
[4] *Institute of High Energy Physics, Beijing, People's Republic of China*
[5] *Universidad de los Andes, Bogotá, Colombia*
[6] *Charles University, Center for Particle Physics, Prague, Czech Republic*
[7] *Institute of Physics, Academy of Sciences, Center for Particle Physics, Prague, Czech Republic*
[8] *Universidad San Francisco de Quito, Quito, Ecuador*
[9] *Institut des Sciences Nucléaires, IN2P3-CNRS, Universite de Grenoble 1, Grenoble, France*
[10] *CPPM, IN2P3-CNRS, Université de la Méditerranée, Marseille, France*
[11] *Laboratoire de l'Accélérateur Linéaire, IN2P3-CNRS, Orsay, France*
[12] *LPNHE, Universités Paris VI and VII, IN2P3-CNRS, Paris, France*

[13] *DAPNIA/Service de Physique des Particules, CEA, Saclay, France*
[14] *Universität Mainz, Institut für Physik, Mainz, Germany*
[15] *Panjab University, Chandigarh, India*
[16] *Delhi University, Delhi, India*
[17] *Tata Institute of Fundamental Research, Mumbai, India*
[18] *Seoul National University, Seoul, Korea*
[19] *CINVESTAV, Mexico City, Mexico*
[20] *FOM-Institute NIKHEF and University of Amsterdam/NIKHEF, Amsterdam, The Netherlands*
[21] *University of Nijmegen/NIKHEF, Nijmegen, The Netherlands*
[22] *Institute of Nuclear Physics, Kraków, Poland*
[23] *Joint Institute for Nuclear Research, Dubna, Russia*
[24] *Institute for Theoretical and Experimental Physics, Moscow, Russia*
[25] *Moscow State University, Moscow, Russia*
[26] *Institute for High Energy Physics, Protvino, Russia*
[27] *Lancaster University, Lancaster, United Kingdom*
[28] *Imperial College, London, United Kingdom*
[29] *University of Arizona, Tucson, Arizona 85721*
[30] *Lawrence Berkeley National Laboratory and University of California, Berkeley, California 94720*
[31] *University of California, Davis, California 95616*
[32] *California State University, Fresno, California 93740*
[33] *University of California, Irvine, California 92697*
[34] *University of California, Riverside, California 92521*
[35] *Florida State University, Tallahassee, Florida 32306*
[36] *Fermi National Accelerator Laboratory, Batavia, Illinois 60510*
[37] *University of Illinois at Chicago, Chicago, Illinois 60607*
[38] *Northern Illinois University, DeKalb, Illinois 60115*
[39] *Northwestern University, Evanston, Illinois 60208*
[40] *Indiana University, Bloomington, Indiana 47405*
[41] *University of Notre Dame, Notre Dame, Indiana 46556*
[42] *Iowa State University, Ames, Iowa 50011*
[43] *University of Kansas, Lawrence, Kansas 66045*
[44] *Kansas State University, Manhattan, Kansas 66506*
[45] *Louisiana Tech University, Ruston, Louisiana 71272*
[46] *University of Maryland, College Park, Maryland 20742*
[47] *Boston University, Boston, Massachusetts 02215*
[48] *Northeastern University, Boston, Massachusetts 02115*
[49] *University of Michigan, Ann Arbor, Michigan 48109*
[50] *Michigan State University, East Lansing, Michigan 48824*
[51] *University of Nebraska, Lincoln, Nebraska 68588*
[52] *Columbia University, New York, New York 10027*
[53] *University of Rochester, Rochester, New York 14627*
[54] *State University of New York, Stony Brook, New York 11794*
[55] *Brookhaven National Laboratory, Upton, New York 11973*
[56] *Langston University, Langston, Oklahoma 73050*
[57] *University of Oklahoma, Norman, Oklahoma 73019*

[58] *Brown University, Providence, Rhode Island 02912*
[59] *University of Texas, Arlington, Texas 76019*
[60] *Texas A&M University, College Station, Texas 77843*
[61] *Rice University, Houston, Texas 77005*
[62] *University of Virginia, Charlottesville, Virginia 22901*
[63] *University of Washington, Seattle, Washington 98195*

Abstract

The central inclusive jet cross section has been measured using a successive-combination algorithm for reconstruction of jets. The measurement uses 87.3 pb^{-1} of data collected with the DØ detector at the Fermilab Tevatron $p\overline{p}$ Collider during 1994–1995. The cross section, reported as a function of transverse momentum ($p_T > 60$ GeV) in the central region of pseudorapidity ($|\eta| < 0.5$), exhibits reasonable agreement with next-to-leading order QCD predictions, except at low p_T where the agreement is marginal.

Jet production in hadronic collisions is understood within the framework of Quantum Chromodynamics (QCD) as a hard scattering of constituent partons (quarks and gluons), that, having undergone the interaction, manifest themselves as showers of collimated particles called jets. Jet finding algorithms associate clusters of these particles into jets so that the kinematic properties of the hard-scattered partons can be inferred and thereby compared to predictions from perturbative QCD (pQCD).

Historically, only cone algorithms have been used to reconstruct jets at hadron colliders [1]. Although well-suited to the understanding of the experimental systematics present in the complex environment of hadron colliders, the cone algorithms used in previous measurements by the Fermilab Tevatron experiments [2,3] present several difficulties: an arbitrary procedure must be implemented to split and merge overlapping calorimeter cones, an ad-hoc parameter, $\mathcal{R}_{\rm sep}$ [4], is required to accommodate the differences between jet definitions at the parton and detector levels, and improved theoretical predictions calculated at the next-to-next-to-leading-order (NNLO) in pQCD are not infrared safe, but exhibit sensitivity to soft radiation [5].

A second class of jet algorithms, which does not suffer from these shortcomings, has been developed by several groups [6–8]. These recombination algorithms successively merge pairs of nearby objects (partons, particles, or calorimeter towers) in order of increasing relative transverse momentum. A single parameter, D, which approximately characterizes the size of the resulting jets, determines when this merging stops. No splitting or merging is involved because each object is uniquely assigned to a jet. There is no need to introduce any ad-hoc parameters, because the same algorithm is applied at the theoretical and experimental level. Furthermore, by design, clustering algorithms are infrared and collinear safe to all orders of calculation. In this Letter, we present the first measurement of the inclusive jet cross section using the $k_\perp$ algorithm [6–9] to reconstruct jets at the $\sqrt{s} = 1.8$ TeV Tevatron proton-antiproton collider.

The differential jet cross section was measured in bins of p_T and pseudorapidity, $\eta \equiv -\ln[\tan(\theta/2)]$, where θ is the polar angle relative to the z axis pointing in the proton beam direction. The $k_\perp$ algorithm implemented at DØ [9] is based on the clustering algorithm suggested in Ref. [8]. The algorithm starts with a list of objects. For each object with transverse momentum $p_{T,i}$, we define $d_{ii} = p_{T,i}^2$, and for each pair of objects, $d_{ij} = \min(p_{T,i}^2, p_{T,j}^2)\,(\Delta R_{i,j})^2/D^2$, where D is the free parameter of the algorithm and $(\Delta R_{i,j})^2 = (\Delta\phi_{ij})^2 + (\Delta\eta_{ij})^2$ is the square of their angular separation. If the minimum of all d_{ii} and d_{ij} is a d_{ij}, then the objects i and j are combined, becoming the merged four-vector $(E_i + E_j,\, \vec{p}_i + \vec{p}_j)$. If the minimum is a d_{ii}, the object i is defined as a jet and removed from subsequent iterations. This procedure is repeated until all objects are combined into jets. Thus $k_\perp$ jets do not have to include all objects in a cone of radius D, and they may include objects outside of this cone.

The primary tool for jet detection at DØ is the liquid-argon/uranium calorimeter [10], which has nearly full solid-angle coverage for $|\eta| < 4.1$. The first stage (hardware) trigger selected inelastic collisions as defined by signal coincidence in the hodoscopes located near the beam axis on both sides of the interaction region. The next stage required energy deposition in any $\Delta\eta \times \Delta\phi = 0.8 \times 1.6$ region of the calorimeter corresponding to a transverse energy (E_T) above a preset threshold. Selected events were digitized and sent to an array of processors. At this stage jet candidates were reconstructed with a cone algorithm (with

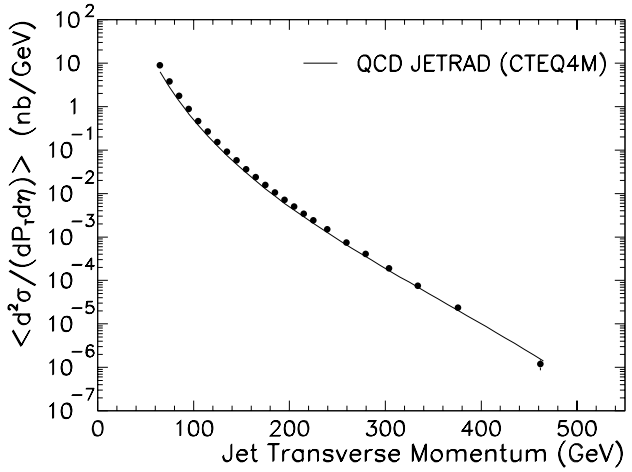

FIG. 1. The central ($|\eta| < 0.5$) inclusive jet cross section obtained with the $k_\perp$ algorithm at $\sqrt{s} = 1.8$ TeV. Only statistical errors are included. The solid line shows a prediction from NLO pQCD.

radius $R \equiv [(\Delta\eta)^2 + (\Delta\phi)^2]^{\frac{1}{2}} = 0.7$), and the event was recorded if any jet E_T exceeded a specified threshold. Jet E_T thresholds of 30, 50, 85, and 115 GeV accumulated integrated luminosities of 0.34, 4.46, 51.5, and 87.3 pb^{-1}, respectively [11].

Jets were reconstructed offline using the $k_\perp$ algorithm, with $D = 1.0$. This value of D was chosen because, at next-to-leading-order (NLO), it produces a theoretical cross section that is essentially identical to the cone prediction for $R = 0.7$ [8], which DØ used in its previous publications on jet production [2]. The vertices of the events were reconstructed using the central tracking system [10]. A significant portion of the data was taken at high instantaneous luminosity, where more than one interaction per beam crossing was probable. When an event had more than one reconstructed vertex, the quantity $S_T = |\Sigma \vec{p}_T^{\,\rm jet}|$ was defined for the two vertices that had the largest numbers of associated tracks, and the vertex with the smallest S_T was used for calculating all kinematic variables [2,11]. To preserve the pseudo-projective nature of the DØ calorimeter, the vertex z-position was required to be within 50 cm of the center of the detector. This requirement rejected $(10.6 \pm 0.1)\%$ of the events, independent of jet transverse momentum.

Isolated noisy calorimeter cells were suppressed with online and offline algorithms [11]. Background introduced by electrons, photons, detector noise, and accelerator losses that mimicked jets were eliminated with jet quality cuts. The efficiency of the jet selection is approximately 99.5% and nearly independent of jet p_T. The imbalance in transverse momentum, "missing transverse energy," was calculated from the vector sum of the $E_{x,y}$ values in all cells of the calorimeter. Background from cosmic rays or incorrectly vertexed events was eliminated by requiring the missing transverse energy in each event to be less than 70% of the p_T of the leading jet. This criterion caused essentially no loss in efficiency.

The DØ jet momentum calibration [9], applied on a jet-by-jet basis, corrects on average the reconstructed calorimeter jet p_T to that of the final-state particles in the jet. The correction accounts for contribution from background from spectator partons (the "underlying-

p_T Bin (GeV)	Plotted p_T (GeV)	Cross Sec. ± Stat. (nb/GeV)	Systematic Uncer. (%)
$60-70$	64.6	$(8.94 \pm 0.06) \times 10^{0}$	$-13, +14$
$70-80$	74.6	$(3.78 \pm 0.04) \times 10^{0}$	$-13, +14$
$80-90$	84.7	$(1.77 \pm 0.02) \times 10^{0}$	$-13, +14$
$90-100$	94.7	$(8.86 \pm 0.25) \times 10^{-1}$	$-13, +14$
$100-110$	104.7	$(4.68 \pm 0.04) \times 10^{-1}$	$-14, +14$
$110-120$	114.7	$(2.68 \pm 0.03) \times 10^{-1}$	$-14, +14$
$120-130$	124.8	$(1.53 \pm 0.02) \times 10^{-1}$	$-14, +14$
$130-140$	134.8	$(9.19 \pm 0.16) \times 10^{-2}$	$-14, +14$
$140-150$	144.8	$(5.77 \pm 0.12) \times 10^{-2}$	$-14, +14$
$150-160$	154.8	$(3.57 \pm 0.03) \times 10^{-2}$	$-15, +14$
$160-170$	164.8	$(2.39 \pm 0.02) \times 10^{-2}$	$-15, +14$
$170-180$	174.8	$(1.56 \pm 0.02) \times 10^{-2}$	$-15, +14$
$180-190$	184.8	$(1.05 \pm 0.02) \times 10^{-2}$	$-15, +14$
$190-200$	194.8	$(7.14 \pm 0.13) \times 10^{-3}$	$-16, +15$
$200-210$	204.8	$(4.99 \pm 0.08) \times 10^{-3}$	$-16, +15$
$210-220$	214.8	$(3.45 \pm 0.07) \times 10^{-3}$	$-16, +15$
$220-230$	224.8	$(2.43 \pm 0.06) \times 10^{-3}$	$-16, +15$
$230-250$	239.4	$(1.50 \pm 0.03) \times 10^{-3}$	$-17, +16$
$250-270$	259.4	$(7.52 \pm 0.23) \times 10^{-4}$	$-17, +16$
$270-290$	279.5	$(4.07 \pm 0.17) \times 10^{-4}$	$-18, +17$
$290-320$	303.8	$(1.93 \pm 0.09) \times 10^{-4}$	$-18, +18$
$320-350$	333.9	$(7.61 \pm 0.59) \times 10^{-5}$	$-19, +19$
$350-410$	375.8	$(2.36 \pm 0.23) \times 10^{-5}$	$-20, +21$
$410-560$	461.8	$(1.18 \pm 0.33) \times 10^{-6}$	$-23, +27$

TABLE I. Inclusive jet cross section of jets reconstructed using the $k_\perp$ algorithm in the central pseudorapidity region ($|\eta| < 0.5$).

event," determined from minimum-bias events), additional interactions, pileup from previous $p\overline{p}$ crossings, noise from uranium radioactivity, detector non-uniformities, and for the global response of the detector to hadronic jets. Unlike the cone algorithm, the $k_\perp$ algorithm does not require additional corrections for showering in the calorimeter [9]. For $|\eta| < 0.5$, the mean total multiplicative correction factor to an observed $p_T$of 100 (400) GeV is 1.094 ± 0.015 (1.067 ± 0.020).

The inclusive jet cross section for $|\eta| < 0.5$ was calculated over four ranges of transverse momentum, each using data from only a single trigger threshold. The more restrictive trigger was used as soon as it became fully efficient. The average differential cross section for each p_T bin, $d^2\sigma/(dp_T d\eta)$, was measured as $N/(\Delta\eta \Delta p_T \epsilon L)$, where $\Delta\eta$ and Δp_T are the η and p_T bin sizes, N is the number of jets observed in that bin, ϵ is the overall efficiency for jet and event selection, and L represents the integrated luminosity of the data sample.

The measured cross section is distorted in p_T by the momentum resolution of the DØ calorimeter. The fractional momentum resolution was determined from the imbalance in p_T in two-jet events [11]. Although the resolution in jet p_T is essentially Gaussian, the steepness of the p_T spectrum shifts the observed cross section to larger values. At 100 (400) GeV, the fractional resolution is 0.061 ± 0.006 (0.039 ± 0.003). The distortion in the cross section due to the resolution was corrected by assuming an ansatz function, $A\, p_T^{-B}(1 - 2\, p_T/\sqrt{s}\,)^C$, smearing it with the measured resolution, and fitting the parameters A, B and C so as to best describe the observed cross section. The bin-to-bin ratio of the original ansatz to the smeared one was used to remove the distortion due to resolution. The unsmearing correction reduces the observed cross section by $(5.7 \pm 1)\%$ $((6.1 \pm 1)\%)$ at 100 (400) GeV.

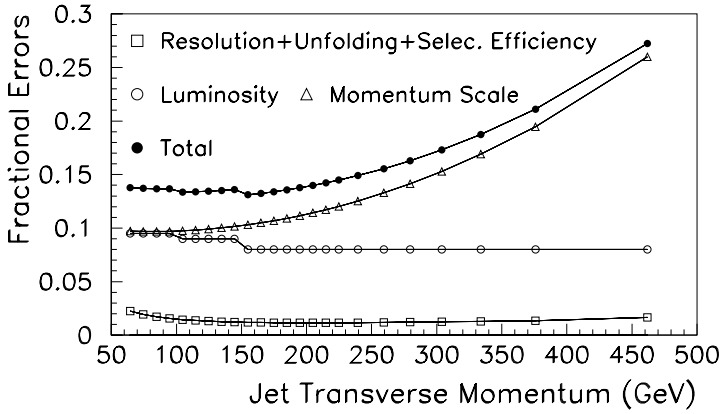

FIG. 2. Fractional experimental uncertainties on the cross section. The discontinuities in the luminosity uncertainty are related to the use of different triggers [11].

PDF	χ^2	χ^2/dof	Probability (%)
MRST	26.8	1.12	31
MRSTg↑	33.1	1.38	10
MRSTg↓	28.2	1.17	25
CTEQ3M	37.5	1.56	4
CTEQ4M	31.2	1.30	15
CTEQ4HJ	27.2	1.13	29
MRST+Hadroniz.	24.0	1.00	46
CTEQ4HJ+Hadroniz.	24.3	1.01	44

TABLE II. χ^2 comparison (24 degrees of freedom) between JETRAD, with renormalization and factorization scales set to $p_T^{\max}/2$, and data for various PDFs. The last entries include a hadronization correction obtained from HERWIG (see text).

The final, fully corrected cross section for $|\eta| < 0.5$ is shown in Fig. 1, along with the statistical uncertainties. Listed in Table I are the p_T range, the best p_T bin centroid, the cross section, and uncertainties in each bin. The systematic uncertainties include contributions from jet and event selection, unsmearing, luminosity, and the uncertainty in the momentum scale, which dominates at all transverse momenta. The fractional uncertainties for the different components are plotted in Fig. 2 as a function of the jet transverse momentum.

The results are compared to the pQCD NLO prediction from JETRAD [12], with the renormalization and factorization scales set to $p_T^{\max}/2$, where $p_T^{\max}$ refers to the p_T of the leading jet in an event. The comparisons are made using parametrizations of the parton distribution functions (PDFs) of the CTEQ [13] and MRST [14] families. Figure 3 shows the ratios of (data-theory)/theory. The predictions lie below the data by about 50% at the lowest p_T and by $(10-20)$% for $p_T > 200$ GeV. To quantify the comparison in Fig. 3, the fractional systematic uncertainties are multiplied by the predicted cross section, and a χ^2 comparison, using the full correlation matrix, is carried out [2]. The results are shown in Table II. Though the agreement is reasonable (χ^2/dof ranges from 1.56 to 1.12, the probabilities from 4 to 31%), the differences in normalization and shape, especially at low p_T, are quite large. The points at low p_T have the highest impact on the χ^2. If the first

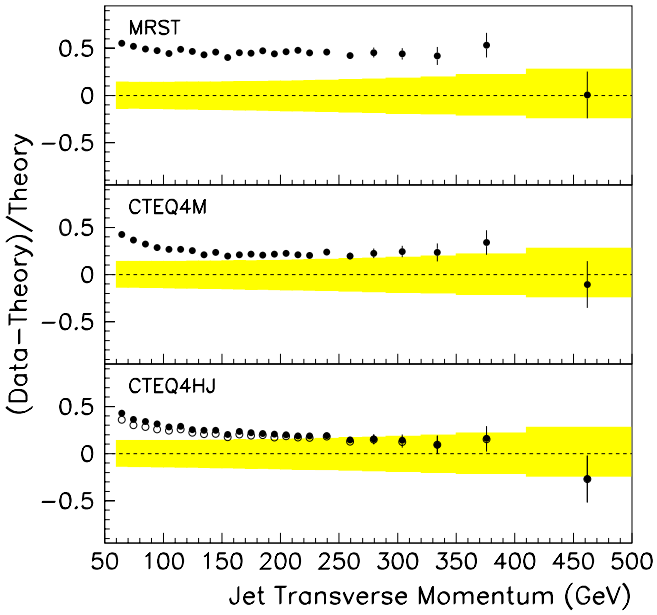

FIG. 3. Difference between data and JETRAD pQCD, normalized to the predictions. The shaded bands represent the total systematic uncertainty. In the bottom plot a HERWIG hadronization contribution has been added to the prediction (open circles).

four data points are not used in the χ^2 comparison, the probability increases from 29% to 77% when using the CTEQ4HJ PDF.

While the NLO predictions for the inclusive cross section for $k_\perp$ ($D = 1.0$) and cone jets ($R = 0.7$, $\mathcal{R}_{\rm sep}$= 1.3 in the same $|\eta| < 0.5$ interval are within 1% of each other for the p_T range of this analysis [11], the measured cross section using $k_\perp$ is 37% (16%) higher than the previously reported cross section using the cone algorithm [15] at 60 (200) GeV. This difference in the cross sections is consistent with the measured difference in p_T for cone jets matched in $\eta - \phi$ space to $k_\perp$ jets. $k_\perp$ jets were found to encompass 7% (3%) more transverse energy at 60 (200) GeV than cone jets [9,11].

The effect of final-state hadronization on reconstructed energy, which might account for the discrepancy between the observed cross section using $k_\perp$ and the NLO predictions at low p_T, and also for the difference between the $k_\perp$ and cone results, was studied using HERWIG (version 5.9) [16] simulations. Figure 4 shows the ratio of p_T spectra for particle-level to parton-level jets, for both the $k_\perp$ and cone algorithms. Particle cone jets, reconstructed from final state particles (after hadronization), have less p_T than the parton jets (before hadronization), because of energy loss outside the cone. In contrast, $k_\perp$ particle jets are more energetic than their progenitors at the parton level, due to the merging of nearby partons into a single particle jet. Including the hadronization effect derived from HERWIG in the NLO JETRAD prediction improves the χ^2 probability from 29% to 44% (31% to 46%) when using the CTEQ4HJ (MRST) PDF. We have also investigated the sensitivity of the measurement to the modeling of the background from spectator partons through the use of minimum bias events, and found that it has a small effect on the cross section: at low p_T,

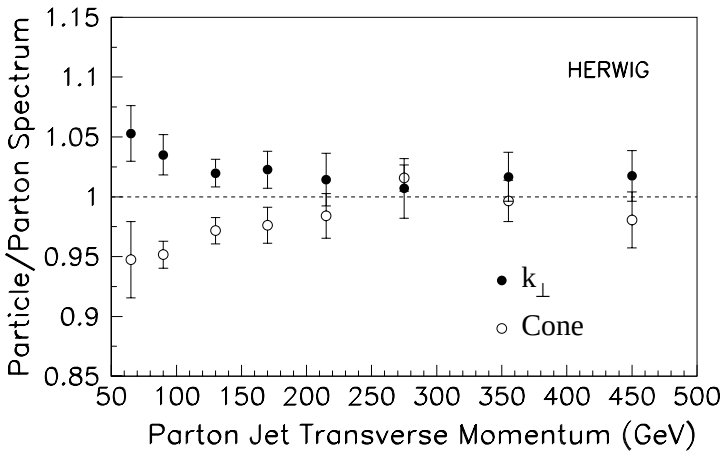

FIG. 4. Ratio of particle-level over parton-level HERWIG p_T spectra for jets, as a function of the parton jet transverse momentum.

where the sensitivity is the largest, an increase of as much as 50% in the underlying event correction decreases the cross section by less than 6%.

In conclusion, we have presented the first measurement in proton-antiproton collisions at $\sqrt{s} = 1.8$ TeV of the inclusive jet cross section using the $k_\perp$ algorithm. Quantitative tests show reasonable agreement between data and NLO pQCD predictions, except at low p_T where the agreement is marginal. Although NLO pQCD theory predicts similar cross sections for jets reconstructed with cone ($R = 0.7$) and $k_\perp$ ($D = 1.0$) algorithms, we find the measurement for $k_\perp$ to lie above the result published for the cone algorithm [2]. This difference is partially explained by incorporating a hadronization contribution of the kind predicted by HERWIG, which also improves the agreement between data and NLO pQCD predictions.

We thank the staffs at Fermilab and collaborating institutions, and acknowledge support from the Department of Energy and National Science Foundation (USA), Commissariat à L'Energie Atomique and CNRS/Institut National de Physique Nucléaire et de Physique des Particules (France), Ministry for Science and Technology and Ministry for Atomic Energy (Russia), CAPES and CNPq (Brazil), Departments of Atomic Energy and Science and Education (India), Colciencias (Colombia), CONACyT (Mexico), Ministry of Education and KOSEF (Korea), CONICET and UBACyT (Argentina), The Foundation for Fundamental Research on Matter (The Netherlands), PPARC (United Kingdom), Ministry of Education (Czech Republic), and the A.P. Sloan Foundation.

REFERENCES

* Visitor from University of Zurich, Zurich, Switzerland.
† Visitor from Institute of Nuclear Physics, Krakow, Poland.

[1] J. Huth *et al.*, in *Proc. of Research Directions for the Decade, Snowmass 1990*, edited by E.L. Berger (World Scientific, Singapore, 1992).
[2] B. Abbott *et al.* (DØ Collaboration), Phys. Rev. D **64** 032003 (2001).
[3] T. Affolder *et al.* (CDF Collaboration), Phys. Rev. D **64** 032001 (2001).
[4] S.D. Ellis, Z. Kunszt and D.E. Soper, Phys. Rev. Lett. **69** , 3615 (1992).
[5] W.T. Giele and W.B. Kilgore, Phys. Rev. D **55** 7183 (1997).
[6] S. Catani, Yu.L. Dokshitzer, M.H. Seymour, and B.R. Webber, Nucl. Phys. **B406** 187 (1993).
[7] S. Catani, Yu.L. Dokshitzer, and B.R. Webber, Phys. Lett. B **285** 291 (1992).
[8] S.D. Ellis and D.E. Soper, Phys. Rev. D **48** 3160 (1993).
[9] V.M. Abazov *et al.* (DØ Collaboration), hep-ex/0108054, submitted to Phys. Rev. D (2001).
[10] S. Abachi *et al.* (DØ Collaboration), Nucl. Instr. Meth. Phys. in Res. A **338**, 185 (1994).
[11] S. Grinstein, Ph.D. thesis, Univ. de Buenos Aires, Argentina, 2001 (in preparation).
[12] W.T. Giele, E.W.N. Glover, and D.A. Kosower, Phys. Rev. Lett. **73** , 2019 (1994).
[13] H.L. Lai *et al.*, Phys. Rev. D **55**, 1280 (1997).
[14] A. D. Martin *et al.*, Eur. Phys. J. C **4**, 463 (1998).
[15] B. Abbott *et al.* (DØ Collaboration), Phys. Rev. Lett. **86** 1707 (2001).
[16] G. Marchesini *et al.*, Computer Phys. Commun. **67**, 465 (1992).